Electromagnetic Coupling of Coplanar Waveguides and Microstrip Lines to Highly Lossy Dielectric Media

MAGDY F. ISKANDER, SENIOR MEMBER, IEEE, AND THOMAS S. LIND

Abstract—**In medical diagnosis and geophysical well-logging applications of electromagnetic (EM) techniques, it is of critical importance to couple the EM energy to the object under interrogation efficiently and with minimum external leakage. Experimentally, a family of coplanar waveguides and microstrip lines has proven to be ideal EM energy couplers for such applications. To date, no analytical work has been done to investigate the coupling characteristics of these structures to highly lossy dielectric media.**

In this paper, the spectral-domain technique is utilized to analyze the coupling characteristics of coplanar waveguides and microstrip lines to multilayer lossy dielectric media. Numerical results illustrating the dispersion characteristics of coplanar and microstrip lines, as well as the various electric field components coupled to highly lossy dielectric media, are presented. It is shown that the presence of a superstrate of lossless dielectric between the coplanar waveguide and the lossy medium plays a key role in setting up an axial electric field component that facilitates leaky-wave-type coupling to the lossy medium. The thickness of the superstrate relative to the gap width in the coplanar waveguide is important in controlling the magnitude of this axial electric field component. It is also shown that even a very thin superstrate layer would generate the leaky-wave type axial electric field component in the lossy medium. The coupling characteristics of the microstrip and coplanar lines are compared, and results generally show improved coupling if coplanar waveguides were utilized. Specifically, values of the attenuation constant α are higher for coplanar waveguide than for microstrip line, and for both structures, α decreases with the frequency decrease. These, as well as other observations, are illustrated graphically.

I. Introduction

THE DESIGN and characterization of printed circuit components such as microstrip antennas, microstrip lines, and coplanar waveguides and the analysis of their discontinuity junctions have received considerable attention in recent years [1]–[3]. These printed circuit components constitute basic building blocks in more complex microwave and millimeter-wave integrated circuits and devices. A wide variety of techniques has been used to develop dynamic solutions for these printed circuit elements. In some cases, the effect of small losses in, or the anistropy of, the substrate material were considered [2], [4], [5] as perturbational effects that may or may not substantially alter the performance of these devices.

In many medical and geophysical applications of electromagnetic techniques, on the other hand, a family of printed circuit elements, including coplanar waveguides and microstrip lines, have proven experimentally to be ideal as electromagnetic (EM) coupling devices. In these applications, it is crucial that these devices couple the EM energy efficiently and with minimum external leakage. When microwave methods for measuring changes in lung water content were initially being developed, for example, it was shown that the sensitivity of the technique could be significantly improved if the transmission rather than the reflection coefficient was utilized [6]–[8]. The required transmission coefficient measurement, on the other hand, was seriously handicapped by the leakage of the EM radiation around the human body. Interference of this leakage radiation with the highly attenuated transmitted signal through the human body contributes to a serious reduction in the sensitivity and, hence, the adequacy of the method. With the use of coplanar waveguides as transmitting and receiving devices, the sensitivity of the method was improved and the leakage problem, which is typical of other radiating-type devices, was virtually eliminated. Successful experiments on phantoms and animals were performed and the method is being considered for possible clinical adoption. It may be worth adding that devices such as coplanar waveguide have additional attractive features, including small size, light weight, and easy conformity to the body.

The use of EM techniques in geophysical exploration and well logging provides another example where study of the coupling characteristics of coplanar and microstrip lines may prove vital. Of particular interest is the development of low-frequency and broad-band well-logging tools to improve the depth of investigation within the geophysical formation and to pave the avenue toward broad-band and time-domain well logging. Low-frequency well-logging tools are often sensitive to borehole geometries, while higher frequency, pad-type ones have limited depth of investigation, which is often within the thickness of the mud cake. With the recognition of the desirable EM coupling characteristics of printed circuit coplanar and microstrip lines, there is a great deal of interest in utilizing such devices in well-logging tools [9], [10].

Before these coplanar and microstrip lines can be widely utilized in the above-mentioned medical and geophysical applications, however, their coupling characteristics to

Manuscript received March 31, 1989; revised July 11, 1989.

The authors are with the Department of Electrical Engineering, University of Utah, Salt Lake City, UT 84112.

IEEE Log Number 8930812.

multilayer, lossy dielectric media must be better understood. The various parameters affecting such coupling need to be analyzed and means for controlling and optimizing their performance developed. In this paper, we utilize the spectral-domain method to analyze the coupling characteristics of coplanar waveguide and microstrip line to multilayer lossy dielectric media with complex permittivities as high as those of the human body or the geophysical formation. The analysis procedure, as well as numerical results illustrating the dispersion characteristics and the configuration of the various field components in the lossy medium, will be described in the following sections.

II. Analysis Procedure

The spectral-domain method is used to analyze the coupling characteristics of a coplanar waveguide, a conductor-backed coplanar waveguide, and a microstrip line to multilayer lossy dielectric media. It is also used to analyze the role of a thin layer of lossless superstrate in controlling the coupling characteristics. The spectral-domain method provides an elegant procedure for reducing partial differential equations to ordinary ones, which often can be further simplified analytically. This method has become by far the most popular method for analyzing the propagation characteristics of many microwave and millimeter-wave integrated circuits [11]. To help us identify desirable coupling characteristics, we analyzed three structures, including the four-layer coplanar waveguide, the three-layer conductor-backed coplanar waveguide, and the three-layer microstrip line shown in Fig. 1.

In all geometries given in Fig. 1, layer 2 represents the substrate, while layers 3 and 4 represent the coupling superstrate and the lossy dielectric medium, respectively. For $e^{-j\omega t}$ time-harmonic fields, assuming $e^{\Gamma z}$ propagation in the z direction and taking the Fourier transform with respect to x of the Helmholtz wave equation, we obtain

$$\text{F.T.}\left\{\left(\nabla^2 + k_i^2\right)\overset{e}{\phi}_i^h\right\} = \left(\frac{d^2}{dy^2} + k_i^2 + \Gamma^2 - \tau^2\right)\overset{e}{\tilde{\phi}}_i^h = \left(\frac{d^2}{dy^2} - \gamma_i^2\right)\overset{e}{\tilde{\phi}}_i^h = 0 \tag{1}$$

where $\overset{e}{\tilde{\phi}}_i^h$ is the Fourier transform of the TE and TM potentials $\overset{e}{\phi}_i^h$ in the ith region, $\gamma_i^2 = \tau^2 - \Gamma^2 - k_i^2$, and k_i is the free-space propagation constant in the ith region, given by

$$k_i^2 = \omega^2 \mu_0 \epsilon_i^*.$$

The transform $\overset{e}{\tilde{\phi}}_i^h$ is related to $\overset{e}{\phi}_i^h$ by

$$\overset{e}{\tilde{\phi}}_i^h(\tau, y) = \int_{-\infty}^{\infty} \overset{e}{\phi}_i^h(x, y) e^{-j\tau x}\, dx. \tag{2}$$

Equation (1) is an ordinary differential equation in the transformed scalar potential quantities $\tilde{\phi}_i^{e,h}$. Suitable solution expansions of (1) in the various dielectric regions are then obtained and the electric and magnetic field components in the ith dielectric region are then found in terms of these potential functions by

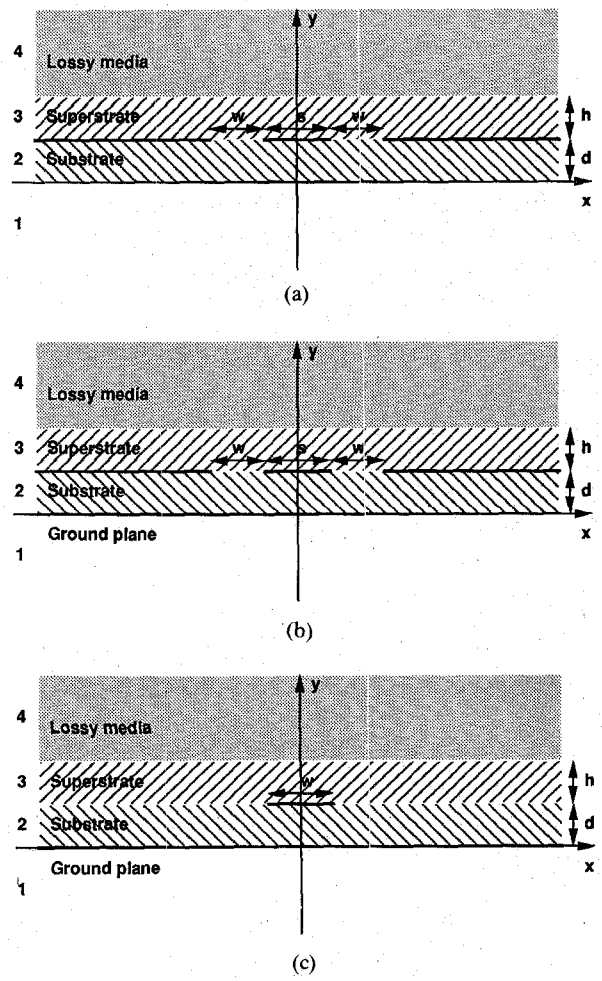

Fig. 1. (a) Four-dielectric-layer coplanar waveguide. (b) Three-dielectric-layer conductor-backed coplanar waveguide. (c) Three-dielectric-layer microstrip line.

$$\tilde{E}_{z,i} = -\frac{k_i^2 + \Gamma^2}{\Gamma}\tilde{\phi}_i^e e^{-\Gamma z} \tag{3a}$$

$$\tilde{H}_{z,i} = -\frac{k_i^2 + \Gamma^2}{\Gamma}\tilde{\phi}_i^h e^{-\Gamma z} \tag{3b}$$

$$\tilde{E}_{t,i} = -\nabla_t \tilde{\phi}_i^e - \frac{j\omega\mu_0}{\Gamma}\bar{i}_z \times \nabla_t \tilde{\phi}_i^h \tag{3c}$$

$$\tilde{H}_{t,i} = \frac{j\omega\epsilon_i}{\Gamma}\bar{i}_z \times \nabla_t \tilde{\phi}_i^e - \nabla_t \tilde{\phi}_i^h \tag{3d}$$

where the subscript t stands for the transverse components of the electric and magnetic fields. Substituting the potential expansions, carrying out a routine differentiation with respect to y, and replacing $\partial/\partial x$ by $(-j\tau)$, we obtain expressions for the electric and magnetic field components in the various regions. By applying the boundary conditions at the interfaces between the various dielectric re-

gions, we obtain a set of coupled equations of the form

$$\begin{bmatrix} G_{11}(\tau,\Gamma) & G_{12}(\tau,\Gamma) \\ G_{21}(\tau,\Gamma) & G_{22}(\tau,\Gamma) \end{bmatrix} \begin{bmatrix} \tilde{E}_x(\tau) \\ \tilde{E}_z(\tau) \end{bmatrix} = \begin{bmatrix} \tilde{J}_x(\tau) \\ \tilde{J}_z(\tau) \end{bmatrix} \quad (4)$$

where $\tilde{E}_x$ and $\tilde{E}_z$ denote the Fourier transforms of the x and z components of the electric field in the slots, while $\tilde{J}_x$ and $\tilde{J}_z$ denote the Fourier transforms of the x- and z-directed current density components on the metal.

Next, either the electric field in the gap or the current density on the metal is expanded in terms of a known set of basis functions. For the coplanar waveguide and the conductor-backed coplanar waveguide, it is more functional to expand the electric field in the gaps, while for the microstrip it is easier to expand the current on the metal strip. To expand the current, (4) must be rearranged to

$$\begin{bmatrix} \tilde{E}_z(\tau) \\ \tilde{E}_x(\tau) \end{bmatrix} = \begin{bmatrix} \dfrac{G_{11}(\tau,\Gamma)}{G_{12}(\tau,\Gamma)G_{21}(\tau,\Gamma)-G_{11}(\tau,\Gamma)G_{22}(\tau,\Gamma)} & \dfrac{G_{21}(\tau,\Gamma)}{G_{12}(\tau,\Gamma)G_{21}(\tau,\Gamma)-G_{11}(\tau,\Gamma)G_{22}(\tau,\Gamma)} \\ -G_{12}(\tau,\Gamma) & -G_{22}(\tau,\Gamma) \\ \dfrac{}{G_{12}(\tau,\Gamma)G_{21}(\tau,\Gamma)-G_{11}(\tau,\Gamma)G_{22}(\tau,\Gamma)} & \dfrac{}{G_{12}(\tau,\Gamma)G_{21}(\tau,\Gamma)-G_{11}(\tau,\Gamma)G_{22}(\tau,\Gamma)} \end{bmatrix} \begin{bmatrix} \tilde{J}_z(\tau) \\ \tilde{J}_x(\tau) \end{bmatrix}. \quad (5)$$

Then, by applying Galerkin's method to (4) or (5), we obtain

$$\sum_{n=1}^{\infty} P_{mn}(\Gamma)a_n + \sum_{n=1}^{\infty} Q_{mn}(\Gamma)b_n = 0 \quad (6a)$$

$$\sum_{n=1}^{\infty} R_{mn}(\Gamma)a_n + \sum_{n=1}^{\infty} S_{mn}(\Gamma)b_n = 0 \quad (6b)$$

where

$$Q_{mn}(\Gamma) = \int_{-\infty}^{\infty} G_{12}(\tau,\Gamma)\tilde{\eta}_m(\tau)\tilde{\xi}_n(\tau)\,d\tau$$

for coplanar waveguides and conductor-backed coplanar waveguides, and

$$Q_{mn}(\Gamma) = \int_{-\infty}^{\infty} \frac{G_{21}(\tau,\Gamma)}{G_{12}(\tau,\Gamma)G_{21}(\tau,\Gamma)-G_{11}(\tau,\Gamma)G_{22}(\tau,\Gamma)} \cdot \tilde{\eta}_m(\tau)\tilde{\xi}_n(\tau)\,d\tau$$

for the microstrip line. The quantities $\tilde{\eta}(\tau)$ and $\tilde{\xi}(\tau)$ are the Fourier transforms of the expansion functions used to express the E_x and E_z components of the fields in the coplanar gap, or the J_z and J_x components of the current density on the microstrip. Similar expressions are obtained for P_{mn}, R_{mn}, and S_{mn} in terms of $\tilde{\eta}_m$, $\tilde{\xi}_n$, and the dydic Green's functions $G_{ij}(\tau,\Gamma)$, $i=1,2$ and $j=1,2$. The propagation constant Γ is obtained by making the determinant of the coefficient matrix (eq. 6) be zero. Spatial-domain expressions of the field components are obtained by taking the inverse Fourier transforms of the spectral domain field expressions given in (3).

The simple one-term expansion given in (7) below was used in our calculations. This expansion function includes the singularity of the E_x field component or the J_z current component at the edges [12]:

$$\eta_1(x) = \begin{cases} \dfrac{1}{\sqrt{\left(\frac{w}{2}\right)^2 - x^2}} & \text{in gaps or on strip} \\ 0 & \text{otherwise} \end{cases} \quad (7a)$$

$$\zeta_1(x) = \begin{cases} x\sqrt{\left(\frac{w}{2}\right)^2 - x^2} & \text{in gaps or on strip} \\ 0 & \text{otherwise.} \end{cases} \quad (7b)$$

After determining the complex propagation constant $\Gamma = \alpha + j\beta$, a suitable zero-finding routine [13] can be used to find ϵ_{eff} and λ from

$$\epsilon_{\text{eff}} = \frac{\beta^2}{k_0^2} \quad (8)$$

$$\lambda = \frac{2\pi}{\beta}. \quad (9)$$

III. Numerical Results

To check the accuracy and convergence of our numerical calculations, we compared the results obtained with dispersion characteristics data available in the literature for coplanar waveguides and microstrip lines. Fig. 2 shows comparisons of some of the obtained dispersion characteristics with data available in the literature [12], [14] for coplanar waveguides. Results for both even and odd modes in coplanar waveguides are in excellent agreement with available data. Fig. 3 shows comparisons of some obtained dispersion characteristics with data available in the literature [5], [15], [16] for the microstrip line. The obtained results are also in excellent agreement, including the case that includes dielectric loss in a lossy substrate microstrip line, as shown in Fig. 3(c).

The conductor-backed coplanar waveguide has been compared to the open coplanar waveguide and the microstrip line by varying the substrate thickness d while the rest of the variables were kept the same. When d is large compared to the gap width w, the conductor-backed coplanar waveguide should have the same dispersion characteristics (e.g., ϵ_{eff}, λ/λ_0) as the open coplanar waveguide.

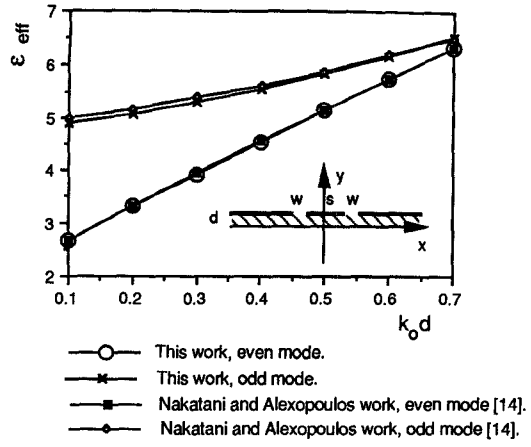

(a)

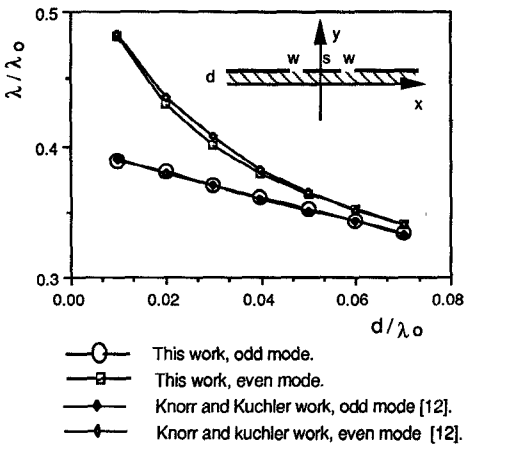

(b)

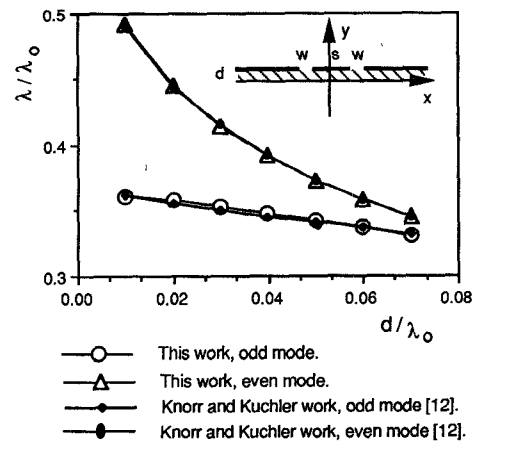

(c)

Fig. 2. Comparison of numerically obtained dispersion characteristics of coplanar waveguide with available data, ϵ_r is the dielectric constant of the substrate. (a) $\epsilon_r = 10.2$, $w/d = 1.0$, $s/d = 0.5$. (b) $\epsilon_r = 16.0$, $w/d = 0.4$, $s/d = 0.3$. (c) $\epsilon_r = 16.0$, $w/d = 0.4$, $s/d = 1.0$.

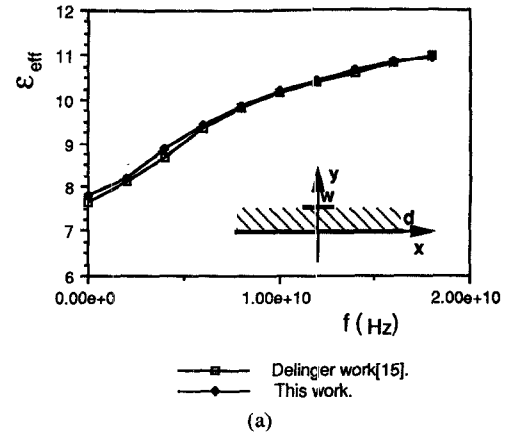

(a)

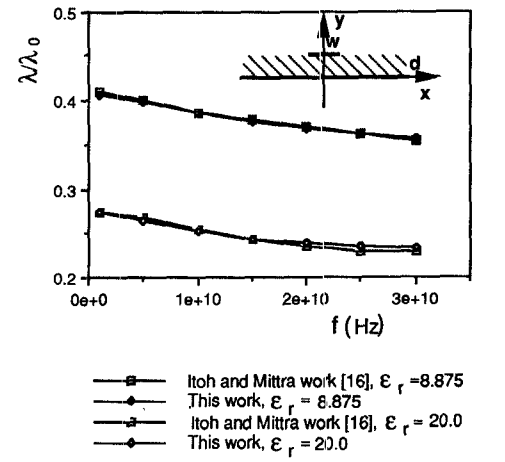

(b)

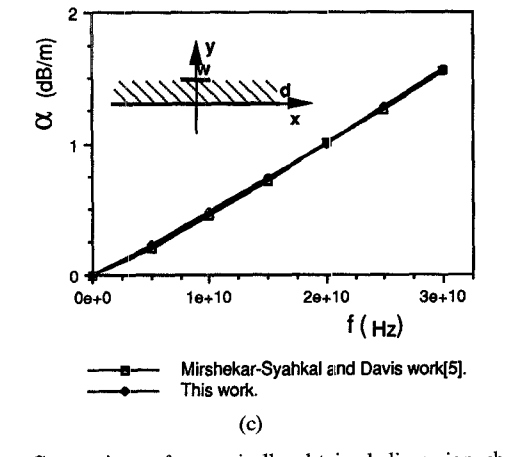

(c)

Fig. 3. Comparison of numerically obtained dispersion characteristics of microstrip line with available data. ϵ_r is the dielectric constant of the substrate. (a) $\epsilon_r = 11.7$, $w/d = 0.96$, $d = 3.17$ mm. (b) $w = d = 1.27$ mm. (c) $w = d = 0.5$ mm, $\epsilon_r = 10$, $\tan\delta = 2.10^{-4}$.

However, when d is small compared to w, the dispersion characteristics for the conductor-backed coplanar waveguide should approach those of the microstrip line. This behavior can be observed in Fig. 4.

After carrying out a large number of comparisons to validate the accuracy of the developed computer code (i.e., Figs. 2–4), results for analyzing the coupling characteristics of microstrip and coplanar lines and investigating the role of a superstrate in controlling such coupling were obtained. First, results for the spatial distribution of the transverse electric field components in coplanar waveguides were calculated and shown in Fig. 5. It is apparent from this figure that the transverse electric field components are much stronger when the coplanar waveguide is placed in direct contact with a high-dielectric-constant lossy medium. These stronger transverse fields thus have

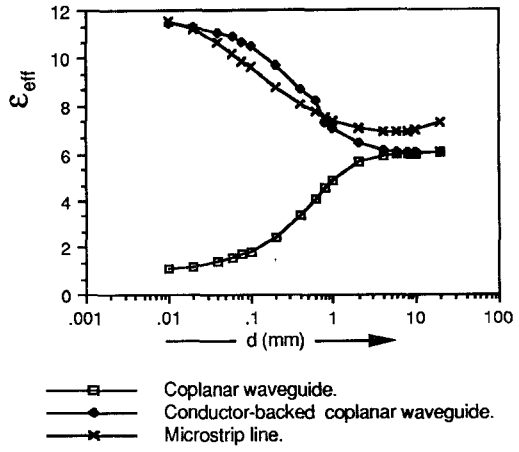

Fig. 4. Comparison between values of ϵ_{eff} for coplanar, conductor-backed coplanar waveguides, and microstrip line versus the substrate thickness d. $w = s = 1$ mm, $\epsilon_r = 11$, and frequency is 1 GHz.

an improved penetration in the high-dielectric material. Of particular interest, however, is the role of a superstrate in controlling the coupling characteristics to the high-dielectric lossy medium. Fig. 6 shows the spatial distribution of the coupled electric field when a layer of lossless dielectric superstrate was placed between the coplanar waveguide and the lossy medium. Numerical results generally showed a significant reduction in the magnitude of the transverse field components in the lossy medium. At the same time, however, a significant increase in the axial component of the electric field, E_z, was observed. This, in effect, reduced the TEM type of wave in the lossy medium and instead facilitated a leaky-wave type of coupling to the lossy medium. Fig. 7 shows the radial attenuation of the axial electric field component for both cases with and without the superstrate. Fig. 8 shows the variation of the normalized magnitude of the axial electric field component versus h/s, where h is the thickness of the superstrate and s is the width of the center conductor in the coplanar waveguide. From this figure it is clear that while a very thin superstrate layer is sufficient to set up the leaky-wave-type axial electric field component, the magnitude of this field decreases rapidly with the increase in the superstrate thickness. This may be explained in terms of the increased ability of the fields to recover the TEM mode type with the increase in the superstrate thickness. A value of $h/s = 1$ may be considered sufficient for recovering the TEM-mode-type propagation. Fig. 8 also shows that the axial electric field component increases with the increase in gap width w. Fig. 9 shows the variation of the attenuation constant α, which is proportional to the coupling efficiency, with the thickness of the superstrate for three different values of the loss tangent of the lossy dielectric medium. It can be seen from this figure that α generally increases with the decrease in h, thus indicating an increased coupling to the lossy medium, and that α also increases with the increase in the loss tangent of the lossy dielectric medium. It should be noted, however, that based on Fig. 8, a reduction in the thickness of the superstrate

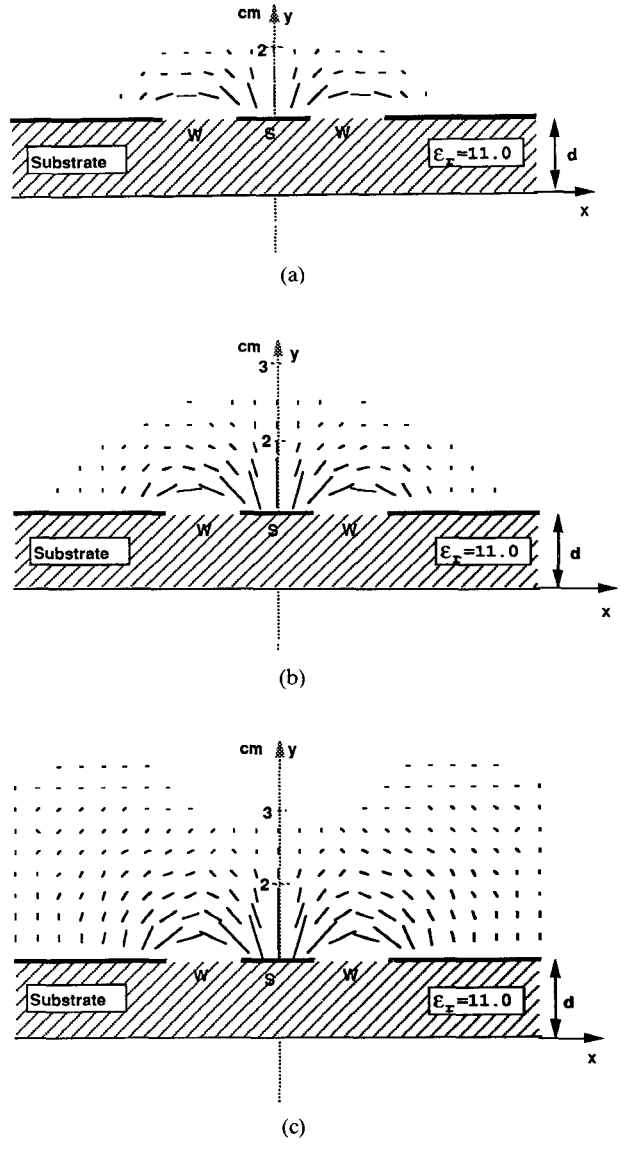

Fig. 5. Spatial distribution of the transverse components of the electric field (a) in air, (b) in lossy dielectric medium of $\epsilon_r = 30 + j20$, and (c) in lossy dielectric medium of $\epsilon_r = 60 + j20$. In all cases, the substrate has an $\epsilon_r = 11$ and a thickness $d = 1$ cm. The widths of the center conductor and the gap are $s = 1$ cm and $w = 1$ cm, respectively. Calculations were made at a frequency of 1 GHz.

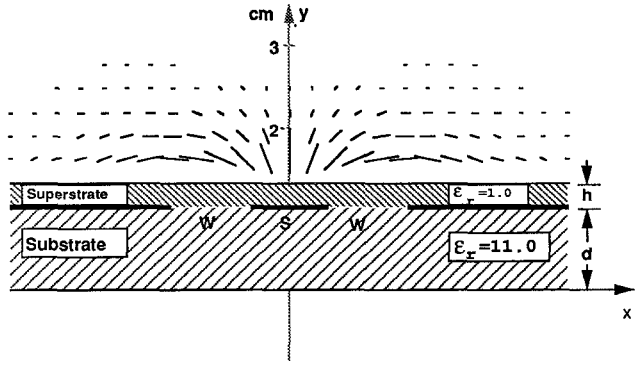

Fig. 6. Spatial distribution of the transverse components of the dielectric field when a superstrate of thickness 0.292 cm was placed between the coplanar waveguide and the lossy dielectric medium of $\epsilon_r = 60 + j20$. All other dimensions and frequency are the same as in Fig. 5.

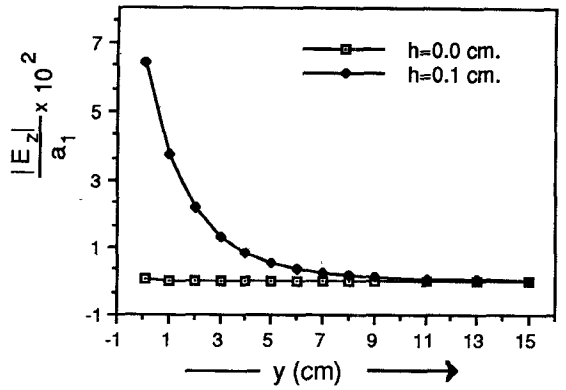

Fig. 7. The magnitude of axial electric-field component $|E_z|$ in a lossy dielectric medium of $\epsilon_r = 60 + j20$ when placed in direct contact with the coplanar waveguide $h = 0$ cm, and when a superstrate of $h = 0.1$ cm was placed between the coplanar waveguide and the lossy medium. Calculations were made along the vertical y axis for $x = 0$. All other dimensions and frequency are the same as in Fig. 5. a_1 is the leading expansion coefficient in eq. (6).

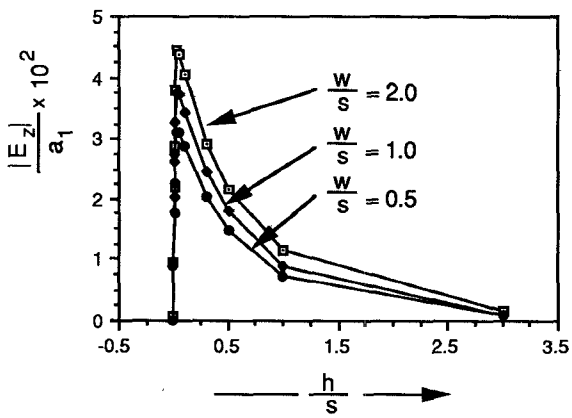

Fig. 8. Variation of the magnitude of the axial field component $|E_z|$ with the relative height of the superstrate layer h/s in a coplanar waveguide. Results are shown for three different values of w/s. The frequency is 1 GHz. $d/s = 1.0$ and $s = 5$ mm. $|E_z|$ is calculated at $x = 0$ and $y = 5$ mm above the substrate. a_1 is the leading expansion coefficient in eq. (6).

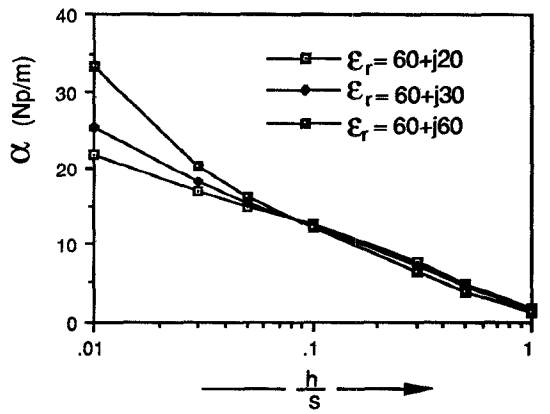

Fig. 9. Variation of the attenuation constant α for a coplanar waveguide with the height of the superstrate layer at 1 GHz. Results are shown for three different values of loss tangent of importance to coupling to human body. Results are given for the case $w/s = d/s = 1.0$, $s = 1.0$ cm.

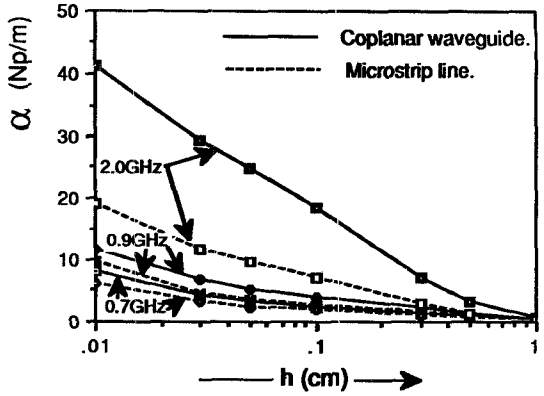

Fig. 10. Comparison between the attenuation constant α for both coplanar waveguide and microstrip line at three frequencies. Results are shown for $w = d = 0.5$ cm for the microstrip and $w = d = s = 0.5$ cm for the coplanar. Dielectric constant of the substrate in both cases $\epsilon_r = 11$, and the complex permittivity of the lossy medium $\epsilon_r^* = 60 + j30$. Superstrate is air filled.

$h < 0.22$ mm would result in a significant reduction in the axial electric field component and, hence, the leaky-wave-type coupling. Fig. 10 shows a comparison between the coupling efficiencies (as indicated by the attenuation constant α) of coplanar and microstrip lines. It can be seen that α is generally larger for the coplanar waveguide; hence this structure is expected to have an improved coupling efficiency. Furthermore, Fig. 10 shows a general trend of decrease in α at lower frequencies and with the increase in the thickness of the superstrate layer.

IV. Comparison with Experimental Data

As indicated in earlier sections, extensive experimental evaluations of the coupling characteristics of coplanar waveguides to lossy dielectric objects have been reported [6]–[8], [17]. It is important at this point to clarify the correlation between available experimental data and the analytical results reported in this paper.

First, it is shown that while a TEM-mode type of propagation is typical in a coplanar waveguide in air at 1 GHz, which is a typical operational frequency in these applications, a significant enhancement in coupling occurs when the coplanar is placed in direct contact with a highly lossy medium. This observation and the fact that the EM coupling is enhanced with the increase in frequency have previously been reported experimentally [7], [8], [17], [18]. In addition, a detailed experimental comparison of the role of the substrate material on controlling the amount of coupling and reducing the leakage radiation was reported in [7]. Specifically, it was shown that reducing the dielectric constant of the substrate, or removing the substrate altogether [7, fig. 2], substantially reduces the leakage radiation and improves the coupling. This same observation may be seen in Fig. 11, where the effect of the dielectric constant of the substrate on the amount of coupling was examined numerically using the spectral-domain approach described in this paper. The results of Fig. 11 confirm the experimental observations reported earlier in [7]. This, as well as the other observations discussed

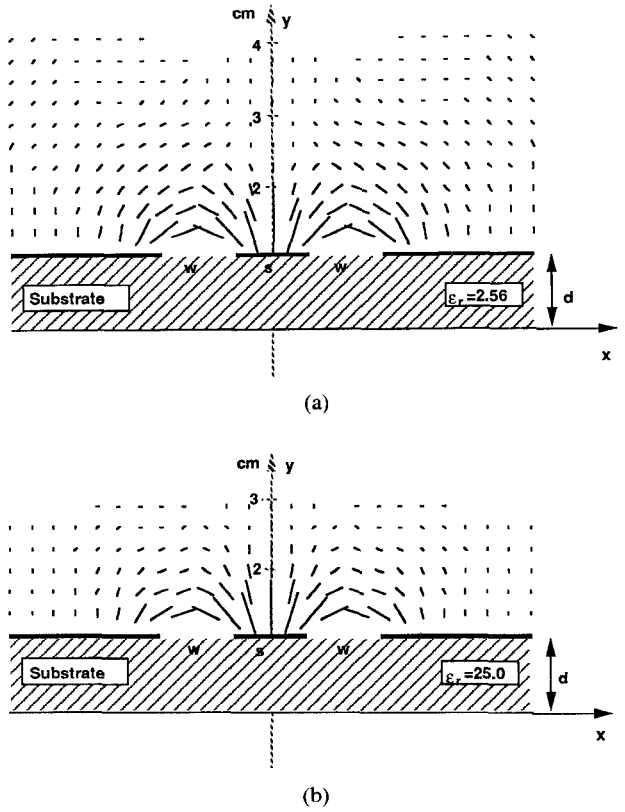

Fig. 11. Spatial distribution of the transverse components of the electric field (a) for a substrate of $\epsilon_{r2} = 2.256$ and (b) for a substrate of $\epsilon_{r2} = 25.0$. In both cases, $w = s = d = 1.0$ cm, a lossy dielectric medium of $\epsilon_{r4} = 60 + j20$, and frequency = 1 GHz.

earlier, shows good correlation between the experimental observations made in earlier publications [6]–[8], [17], [18] and the numerical results reported in this paper.

V. Conclusions

The spectral-domain method is used to analyze the EM leaky-wave-type coupling of microstrip lines and coplanar waveguides to multilayer lossy dielectric media. Detailed analyses of these coupling characteristics and the role of a thin superstrate layer of lossless material in controlling this coupling are important in fully developing the application of printed circuit technology in medical and geophysical applications. The numerical results obtained for the dispersion characteristics of coplanar and microstrip lines when the lossy media were absent were all found to be in excellent agreement with published data. Results were then obtained to describe the spatial field distribution in the lossy medium and the effect of a thin layer of lossless superstrate on controlling the coupling to the lossy medium. It is observed that the superstrate layer generally enhances an axial, leaky-wave-type electric field component, which facilitates strong coupling to the lossy medium. The coupling was found to decrease with the frequency decrease, to increase with the increase of the loss tangent of the lossy medium, and generally to be stronger for the coplanar waveguide than for the microstrip. It is also observed that while a thin superstrate layer is generally sufficient to set up the axial electric field, the magnitude of this field decreases rapidly with the increase in the superstrate thickness. These observations correlate very well with available experimental observations [6]–[8], [17].

References

[1] M. W. Mink and F. R. Schwering, Eds., Special Issue on Numerical Methods, *IEEE Trans. Microwave Theory Tech.*, vol. MTT-33, Oct. 1985.

[2] N. G. Alexopoulos, "Integrated-circuit structures on anisotropic substrates," *IEEE Trans. Microwave Theory Tech.*, vol. MTT-33, pp. 847–881, 1985.

[3] A. K. Sharma, Ed., Special Issue on Quasi-Planar Millimeter-Wave Components and Subsystems, *IEEE Trans. Microwave Theory Tech.*, vol. 37, Feb. 1989.

[4] M. Aubourg, J. P. Vollotee, F. Godon, and Y. Garault, "Finite element analysis of lossy waveguides—Application to microstrip lines on semiconductor substrate," *IEEE Trans. Microwave Theory Tech.*, vol. MTT-31, pp. 326–330, 1983.

[5] D. Mirshekar-Syahkal and J. B. Davis, "Accurate solution of microstrip and coplanar structures for dispersion and for dielectric and conductor losses," *IEEE Trans. Microwave Theory Tech.*, vol. MTT-27, pp. 694–699, 1979.

[6] M. F. Iskander and C. H. Durney, "Electromagnetic energy coupler/receiver: Apparatus and method," U.S. Patent 4 240 445.

[7] M. F. Iskander and C. H. Durney, "Microwave methods of measuring changes in lung water," *J. Microwave Power*, vol. 18, pp. 265–275, 1983.

[8] M. F. Iskander and C. H. Durney, "Electromagnetic techniques for medical diagnostics: A review," *Proc. IEEE*, vol. 68, pp. 126–132, 1980.

[9] M. F. Iskander, S. L. Rattlingourd, and J. Oomrigar, "A new electromagnetic propagation tool for well logging," *Soc. Petroleum Eng.*, publication 13189, 1984.

[10] R. Freedman and J. P. Vogatizis, "Theory of microwave dielectric logging using the electromagnetic wave propagation method," *Geophysics*, vol. 44, pp. 969–986, 1979.

[11] R. H. Jansen, "The spectral-domain approach for microwave integrated circuits," *IEEE Trans. Microwave Theory Tech.*, vol. MTT-33, pp. 847–881, 1985.

[12] J. B. Knorr and K. D. Kuchler, "Analysis of coupled slots and coplanar strips on dielectric substrates," *IEEE Trans. Microwave Theory Tech.*, vol. MTT-23, pp. 541–548, 1975.

[13] Complex zero finding route, "Zanlyt," IMSL-Math/Library, Version 1.0, pp. 767–769, Apr. 1987.

[14] A. Nakatani and N. G. Alexopoulos, "Toward a generalized algorithm for modeling of the dispersive properties of integrated circuit structures on anisotropic substrates," *IEEE Trans. Microwave Theory Tech.*, vol. MTT-33, pp. 1436–1441, 1985.

[15] E. J. Denlinger, "A frequency dependent solution for microstrip transmission lines," *IEEE Trans. Microwave Theory Tech.*, vol. MTT-19, pp. 30–39, 1971.

[16] T. Itoh and R. Mittra, "Spectral domain approach for calculating the dispersion characteristics of microstrip lines," *IEEE Trans. Microwave Theory Tech.*, vol. MTT-21, pp. 496–499, 1973.

[17] M. F. Iskander, C. H. Durney, D. J. Shoff, and D. G. Bragg, "Diagnosis of pulmonary edema by a surgically noninvasive microwave technique," *Radio Sci.*, vol. 14, no. 65, pp. 265–269, 1979.

[18] M. F. Iskander and C. H. Durney, "Electromagnetic energy coupler for medical applications," *Proc. IEEE*, vol. 67, pp. 1463–1465, 1979.

✠

Magdy F. Iskander (S'72–M'76–SM'84) was born in Alexandria, Egypt, on August 6, 1946. He received the B.Sc. degree in electrical engineering from the University of Alexandria, Egypt, in 1969. He received the

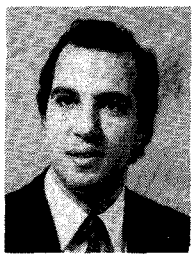

M.Sc. and Ph.D. degrees in 1972 and 1976, respectively, both in microwaves, from the University of Manitoba, Winnipeg, Canada.

In 1976, he was awarded a National Research Council of Canada Postdoctoral Fellowship at the University of Manitoba. Since 1977 he has been with the Department of Electrical Engineering and the Department of Bioengineering at the University of Utah, Salt Lake City, where he is currently a Professor of Electrical Engineering and a Research Professor of Materials Science and Engineering. In 1981, he received the University of Utah President David P. Gardner Faculty Fellow Award and spent the academic quarter on leave as a Visiting Associate Professor at the Department of Electrical Engineering and Computer Science, Polytechnic Institute of New York, Brooklyn. He spent the summers of 1985 and 1986 at the Chevron Oil Field Research Company, La Habra, CA, as Visiting Scientist. From September 1986 to May 1987 he spent a sabbatical leave at UCLA, where he worked on the coupling characteristics of microwave integrated circuits to inhomogeneous media, and at the Harvey Mudd College, where he learned about the engineering clinic program. He spent the last four months of the sabbatical leave with the Ecole Superieure d'Electricite, Gif-Sur-Yvette, France, where he worked on microwave imaging. His present fields of interest include the use of numerical techniques in electromagnetics to calculate scattering by dielectric objects, antenna design for medical applications, microwave integrated circuit design, and the use of microwave methods for material characterization and processing.

Dr. Iskander edited two special issues of the *Journal of Microwave Power*, one on electromagnetics and energy application (March 1983), and the other on electromagnetic techniques in medical diagnosis and imaging (September 1983). The holder of seven patents, he has contributed seven chapters to five research books, published more than 85 papers in technical journals, and made more than 150 presentations at technical conferences. In 1983, he received the College of Engineering Outstanding Teaching Award and the College Patent Award for creative, innovative, and practical invention. In 1984, he was selected by the Utah Section of the IEEE as the Engineer of the Year. In 1984 he received the Outstanding Paper Award from the International Microwave Power Institute, and in 1985 he received the Curtis W. McGraw ASEE National Research Award for outstanding early achievements by a university faculty member. In 1986 Dr. Iskander established the Engineering Clinic Program in the College of Engineering at the University of Utah. Since then the program has attracted 18 research projects from nine different companies throughout the United States. He is also a member of the IEEE AP-S Committee on Education and Director of the NSF/IEEE Committee on the use of computers in electromagnetic education.

✠

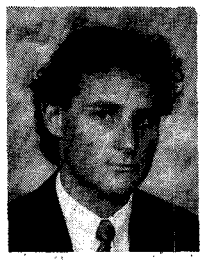

Thomas S. Lind was born in Oslo, Norway, on March 1, 1962. He received the B.S. and M.S. degrees in electrical engineering from the University of Utah, Salt Lake City, in 1987 and 1989, respectively. From 1987 to 1989, he was a research assistant in the Electrical Engineering Department at the University of Utah. In 1983, he obtained a degree in liberal arts from the University of Oslo, Norway. He worked in the Royal Norwegian Army as an officer and instructor in 1981 and 1982. His fields of interest include microwave circuit design with emphasis on numerical techniques.